Dalton Transactions

ROYAL SOCIETY OF CHEMISTRY

PAPER

View Article Online
View Journal | View Issue

Check for updates

Cite this: *Dalton Trans.*, 2026, **55**, 4997

Molybdenum(VI) borano–imido complexes and their application as Lewis acid catalysts in homocoupling of diazo compounds

Karel Škoch, *[a] Michaela Buziková, [a] Michał Jakubczyk, [a] Krishna Pattanamcheril Anilkumar, [a,b] Jan Demel [a] and Miroslava Litecká [a]

We report the synthesis, structural characterization, and catalytic activity of a borano–imido molybdenum complex featuring a unique motif B–N=$MoCl_4$(thf), prepared *via* the reaction of a phenylpyridine-based boron azide with [$MoCl_4$(thf)$_2$]. Spectroscopic and crystallographic analyses confirmed the formation of a linear B–N–Mo(VI) linkage. Reaction of the formed imido complex with various neutral donors resulted in solvent-assisted reduction and formation of several structurally diverse Mo(V) derivatives, showing the adaptability of the imido framework. The Mo(VI) imido complex acts as a strong Lewis acid and efficiently catalyses the homocoupling of diazo compounds under mild conditions. For diaryldiazomethanes, the product selectivity between tetraarylethylenes and azines is primarily governed by the electronic nature of the substituents: electron-donating groups favor the formation of tetraarylethylenes, whereas electron-withdrawing groups lead exclusively to 1,2-bis(diarylmethylene)hydrazines. The complex also mediated the transformation of 1-diazoindenes to afford either 1,1′-biindene or bis(1,2-indenylidene)hydrazines, with the selectivity controlled by steric effects. Furthermore, α-diazophenylacetates were efficiently coupled to yield mixtures of maleates and fumarates, accompanied by minor amounts of azine by-product, with negligible influence of solvent or substituent variation.

Received 24th February 2026,
Accepted 25th February 2026

DOI: 10.1039/d6dt00469e

rsc.li/dalton

Introduction

Organoimido complexes represent a distinct class of compounds featuring a double bond between nitrogen and transition metals.[1] The imido donor $[RN]^{2-}$ is formally a dianionic species that acts as both a σ- and π-donor[2] and its electronic nature, general properties and even the geometry are influenced by the metal centre, its oxidation state, the ancillary ligands and the nature of the R group.[3] These have played a key role in the development of olefin metathesis, for which Robert Schrock was ultimately awarded the Nobel prize.[4] Related compounds can also be encountered as reactive species in diverse nitrogen transfer reactions[5] including diverse aminations,[6] aziridations[7] or nitrogen heterocycle synthesis.[8] Although the role of ancillary ligands in imido chemistry is well established, non-carbon-substituted imido complexes remain scarce. Aside from the more accessible silyl–[9] and phosphanyl–imido[10] species, borano–imido complexes are less explored. Notable examples represent complexes of Ti[11] and Nb[12] derived from tris(pentafluorophenyl)borane-capped nitrido complexes $(C_6F_5)_3$B–N≡[M], together with low-valent Mo species formed *via* hydroboration (or chloroboration) of terminal nitrido complexes.[13] These were systematically investigated and also isolated as key intermediates in molybdenum-mediated dinitrogen reduction.[14]

Recently, we have reported the synthesis of a remarkably robust phenylpyridine boron azide[15] **1**, readily accessible from simple borane $L^{NC}BH_2$ (L^{NC} = 2-phenylpyridine).[16] With this work, we report our investigations on its reactivity towards molybdenum ions, synthesis and reactivity of one-of-a-kind borano–imido complexes and their application as Lewis acid catalysts in the homocoupling of diazo compounds.

Results and discussion

Following the general protocol,[17] boron azide **1** was treated with [$MoCl_4$(thf)$_2$][18] at 75 °C for 5 h to give a deep red complex **2**, which was isolated in 87% yield (Fig. 1). ^{1}H NMR shows signals for the phenylpyridine and cyclopentyl fragments, along with two broad peaks for the coordinated tetrahydrofuran molecule (δ_H = 4.39 and 1.38 ppm). The ^{11}B NMR signal at δ = 8.0 ppm is remarkably high for a tetracoordinate boron, indicating electron density delocalization toward the nitrogen

[a]*Institute of Inorganic Chemistry of the Czech Academy of Sciences, Husinec-Řež 1001, 250 68, Czech Republic. E-mail: skoch@iic.cas.cz*
[b]*Department of Inorganic Chemistry, Faculty of Science, Charles University, Hlavova 2030, 128 40 Prague, Czech Republic*

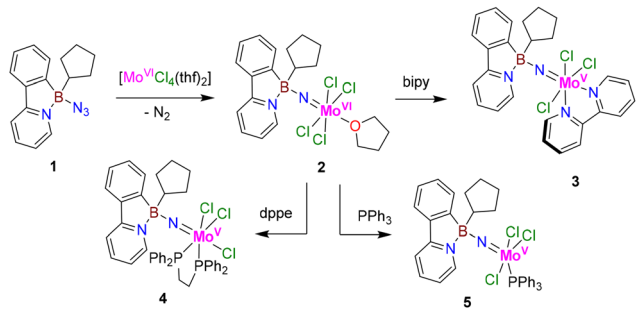

Fig. 1 Synthesis of compound **2** and the derived complexes **3–5**.

atom. The structure of **2** was ultimately confirmed by single-crystal X-ray diffraction analysis, revealing a pseudo-octahedral arrangement on molybdenum, in which the imido fragment and tetrahydrofuran adopt a *trans*-configuration, whereas the axial positions are occupied by chloride anions. The imido-donor atom adopts an almost perfect linear geometry (B–N–Mo angle – 179.3(8)°), while the chloride ligands form a square arrangement slightly tilted toward the tetrahydrofuran molecule (N(2)–Mo–Cl angles ranging from 95° to 99°). The very short N–Mo bond in **2** (1.682(9) Å) lies roughly midway between the typical Ar–N═Mo(VI) imido double bond (~1.72 Å)[19] and the N≡Mo(VI) triple bond (~1.65 Å),[20] indicating a specific donor character of the borano–imido ligand. For the molecular structure, see Fig. 2.

We further explored the reactivity of the imido complex toward different donors. The reaction of **2** with bipyridine (bipy) afforded a grey paramagnetic Mo(V) complex **3**, which confirmed the preservation of the linear geometry of the imido donor, resulting in a pseudo-octahedral geometry in a *mer*-type arrangement with the axial chloride donors once again tilting away from the imidoborane scaffold. A pronounced *trans* effect of the imido donor is observed in the crystal structure, with the Mo–N4 bond over 0.16 Å longer than the Mo–N3 bond. Treatment of **2** with bis(diphenylphosphino)ethane (dppe) gave a poorly soluble orange-red solid compound **4**. Although the quality of SC-XRD data was insufficient for deposition to CCDC database due to the poor crystal quality, the structure clearly reveals the *fac*-isomeric arrangement of the ligands (for the crystal structure model and more details, see the SI). The reaction of **2** with triphenylphosphine, regardless of whether the [Mo]/PPh_3 ratio was 1 : 1 or 1 : 2, led to the formation of a brown complex **5**, in which the pentacoordinate molybdenum forms a tetragonal pyramidal geometry with the imido donor in an apical position. Due to the general low solubility and the paramagnetic nature of Mo(V) (configuration d^1), the obtained complexes were analysed only by EA, HRMS, FTIR and SC-XRD (for the depiction of the crystal structures, see Fig. 2; for details, see the SI).[21]

To gain a deeper insight into the electronic properties of the imido complex **2**, we targeted its isoelectronic fluorene analogue **6**. The detailed synthetic procedure is provided in the SI. Briefly, 9*H*-fluorenone was first reacted with cyclopentyl-

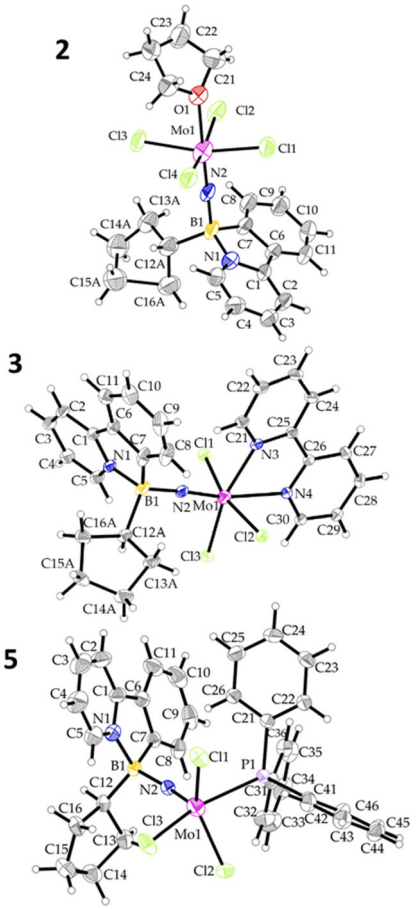

Fig. 2 Crystal structures of complexes **2**, **3** and **5** (asymmetric unit shown, thermal ellipsoids at 30% probability). Selected bond lengths (Å) and angles (°): **2** B1–N2 1.553(2), N2–Mo1 1.682(9), Mo1–O1 2.360(8), B1–N1–Mo1 179.3(8); **3** B1–N2 1.545(5), N2–Mo1 1.692(3), Mo1–N3 2.196(3), Mo1–N4 2.358(3), B1–N2–Mo1 176.5(3), N3–Mo1–N4 71.48(9); **5** B1–N2 1.558(3), N2–Mo1 1.672(2), Mo1–P1 2.5569(5), B1–N2–Mo1 167.4(1), N2–Mo1–P1 93.27(5).

magnesium bromide, and the resulting alcohol was converted into the corresponding azide **6** using $TMSN_3$, and subsequently, compound **6** was treated with $[MoCl_4(thf)_2]$. Unlike the smooth formation of **2**, the reaction of the fluorenyl azide **6** with $[MoCl_4(thf)_2]$ was not selective. Although we cannot rule out the transient formation of the targeted complex, the gradual colour change from reddish-brown to dark green suggested the reduction to Mo(V). Crystallization of the reaction mixture provided a small amount of green crystals of complex **7**. SC-XRD analysis revealed the formation of a dimeric species, in which the pentavalent molybdenum atom coordinates both the imido ligand and a tetrahydrofuran molecule. Its octahedral coordination environment is completed by two terminal and two bridging chloride ligands (see Fig. 3). The resulting coordination environment is therefore analogous to that observed in dimeric molybdenum pentachloride.[22] However, in direct comparison, the geometry of molecule **7** exhibits a noticeable flattening as the Mo–Mo distances are

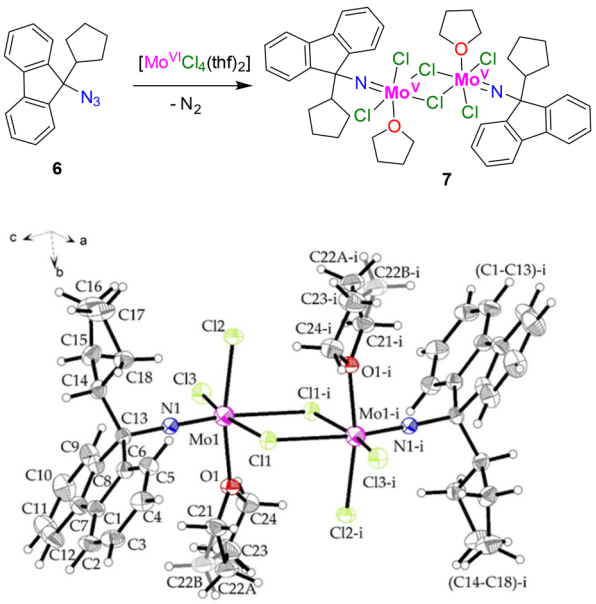

Fig. 3 The preparation and crystal structure of complex **7**. Selected bond lengths (Å) and angles (°): Mo–N1 1.694(2), N1–C13 1.450(3), Mo1–Cl1 2.4505(6), Mo–Cl1i 2.6599(7), Mo–Cl2 2.3549(8), Mo–Cl3 2.3622(7), M1–O1 2.156(2), C13–N1–Mo1 176.8(2).

significantly elongated (3.825(4) Å for compound $MoCl_5$ *vs.* 3.930(2) Å for compound **7**) and the Mo–Cl–Mo angles defined by the bridging chloride bond are widened (98.36(7)° for $MoCl_5$ *vs.* 100.44(2)° for **7**).

Catalytic investigations

Having prepared complex **2**, we next considered its potential application in catalysis. The catalytic chemistry of molybdenum complexes is remarkably broad,[23] but we decided to focus on the fact that **2** features a tetrahydrofuran fragment prone to dissociation, efficiently masking a Lewis-acidic site. Motivated by our previous work on borenium-catalysed diazo homocoupling,[24] we investigated whether **2** could mediate this transformation as efficiently and extend the substrate scope beyond what main-group Lewis acids allow. While related diazo-to-olefin (homo)couplings have been reported for late-transition metals such as rhodium,[25] ruthenium,[26] or copper,[27] to our knowledge this reactivity has not been reported for any early transition metal.

Indeed, under screening conditions (bis-*p*-tolyldiazomethane **8a** as a substrate, 1 mol% catalyst, $CDCl_3$ solvent, 60 min reaction time at room temperature), compound **2** proved catalytically active, affording a complete conversion to the corresponding tetraarylethylene, which was isolated in 95% yield (Table 1, entry 1). In contrast, when the reaction was conducted in aromatic solvents (d_6-benzene), the dominant product was the corresponding azine (bis(*p*-tolylmethylene) hydrazine), isolated in 86% yield (entry 4). We have not previously observed this solvent-dependent selectivity in boron-based catalytic systems (entries 23 and 24). Whereas complexes

Table 1 Solvent and catalyst screening for the Lewis-acid catalysed homocoupling of bis-*p*-tolyldiazomethane

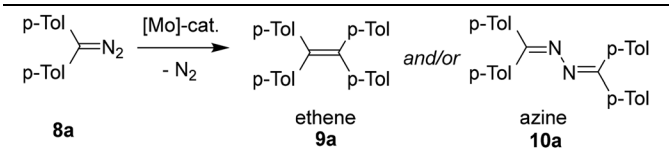

			Conversion[a] (%)	
Entry	Catalyst	Solvent	Ethene **9a**	Azine **10a**
1	**2**	$CDCl_3$	**99(95)**	0
2	**2**	CH_2Cl_2	55	45
3	**2**	Tol	10	90
4	**2**	C_6D_6	5	**95(86)**
5	**2**	Et_2O	<5	20
6	**2**	MTBE	<5	<5
7	**2**	THF	0	0
8	**3**	$CDCl_3$	0	0
9	**3**	C_6D_6	0	0
10	**4**	$CDCl_3$	0	0
11	**4**	C_6D_6	0	0
12	**5**	$CDCl_3$	25	0
13	**5**	C_6D_6	0	20
14[b]	**7**	$CDCl_3$	20	0
15[b]	**7**	C_6D_6	0	20
16	$[MoCl_4(thf)_2]$	$CDCl_3$	15	40
17	$[MoCl_4(thf)_2]$	C_6D_6	0	70
18	$MoCl_5$	$CDCl_3$	60	40
19	$MoCl_5$	C_6D_6	30	55
20	$[MoCl_4(NMes)(thf)]$	$CDCl_3$	80	20
21	$[MoCl_4(NMes)(thf)]$	C_6D_6	10	90
22	$B(C_6F_5)_3$	$CDCl_3$	95	0
23	$B(C_6F_5)_3$	C_6D_6	90	0

Reaction conditions: 0.2 mmol reaction scale, 1 mol% of the catalyst, 1 mL of solvent, 60 minutes at room temperature. [a] Conversion estimated by ^1H NMR (the isolated yields in parentheses are reported for the reaction performed on a 0.5 mmol scale). [b] 0.5 mol% of **7** was used.

3 and **4** were virtually inactive under the screening conditions, complexes **5** and **7** promoted this transformation, albeit with low efficiency. The precursors $MoCl_5$ and $[MoCl_4(thf)_2]$ also catalysed the reaction; both exhibited inferior activity and selectivity compared to catalyst **2**. For comparison, we prepared and evaluated a simple mesitylimido complex $[MoCl_4(NMes)(thf)]$ (see the SI for its synthesis and characterization). While this complex also displayed considerable catalytic activity, it did not exhibit the product selectivity observed for catalyst **2**. The results are summarized in Table 1.

Encouraged by these results, we evaluated catalyst **2** in a broader substrate set comprising both electron-rich and -poor diaryldiazomethanes, diazoindenes and α-diazo esters. Although solvent effects were evident under catalyst screening conditions, the substrate scope showed that the selectivity is predominantly determined by the electronic nature of the diazo compound. Whereas electron-rich diaryldiazomethanes (**8c**, *p*-methoxyphenyl) cleanly afforded the corresponding tetraarylethylene **9** in both $CDCl_3$ and C_6D_6, electron-poor analogues (**8d**, *p*-fluorophenyl and **8e**, *p*-bromophenyl) reacted more slowly, required more forcing conditions (60 °C and

extended reaction times) and produced the corresponding azines **10** exclusively. The very electron-poor **8f** (3,5-bistrifluoromethylphenyl) did not show any signs of any homocoupling product formation.

We further explored the possibility of homocoupling of synthetically accessible 1-diazoindenes.[28] The homocoupling reactions were carried out under more demanding conditions, employing 2 mol% of catalyst **2** and heating to 60 °C. Formation of 1,1′-biindenylidene **9h** (ethylene-type coupling product) was observed only in the case of the simplest 1-diazoindene **8h**; **9h** was isolated as a mixture of *E*- and *Z* isomers in approximately 2 : 1 ratio. In contrast, sterically encumbered 2-methyl- and 2-phenyl-substituted 1-diazoindenes afforded exclusively the corresponding azine products **10i** and **10k**, which were isolated in excellent yields up to 93% regardless of the solvent used.

The less nucleophilic methyl phenyldiazoacetates **8k–m** exhibited different reactivity patterns and generally required harsh reaction conditions (2 mol% of **2**, 5 h at 60 °C) to achieve a full conversion. The main product was an ethylene-type coupling product, giving rise to mixtures of the corresponding 2,3-diphenylmaleate (*Z*-**9**) and 2,3-diphenylfumarate (*E*-**9**) with a slight preference for the *E*-isomer, regardless of the presence of electron-donating (*p*-methoxy) or electron-withdrawing (*p*-bromo) substituents. NMR measurements also revealed the formation of a small amount of the corresponding azines **10k–m**. In some cases, we were able to separate all individual reaction products by column chromatography. Similar to diaryldiazomethanes, the reaction performed in benzene under otherwise identical conditions proceeded worse and did not reach full conversion even after 20 h. On the other hand, the influence of the solvent on the reaction selectivity was marginal (for reaction summary and crystal structures of the selected substrates and products, see Fig. 4 and the SI).

When the catalytic results are compared with those observed for main-group borenium catalysts,[18] it was seen that the borano–imido molybdenum Lewis acid **2** was not as active and required a higher catalyst loading for the homocoupling of diaryldiazomethanes (1% for **2** *versus* 0.1% for the best borenium catalyst). However, complex **2** appears to be more robust and capable of mediating the homocoupling of substrate classes such as α-diazo esters, which generate less nucleophilic carbocation according to Meyr's nucleophilicity scale,[29] and were therefore unreactive in borenium-catalysed reactions.

Finally, we attempted the homocoupling of bis-diazoketone **11**. In the presence of 2 mol% of **2**, a nitrogen molecule was rapidly eliminated to give rise to 2,5-diphenyl-3,4-diazacyclopentadienone (azine-like) intermediate **12**, which immediately underwent a double [3 + 2]-dipolar cyclization to provide a polycyclic trimer-like compound **13** as a sole product (see Fig. 5). It should however be noted that the same outcome was proposed as a product of thermolysis of **11** by Trost.[30] The structure and head-to-tail arrangement of the polycyclic product **13** were ultimately confirmed by SC-XRD.

We expect that the reaction proceeds in a manner analogous to that we previously described for main-group Lewis

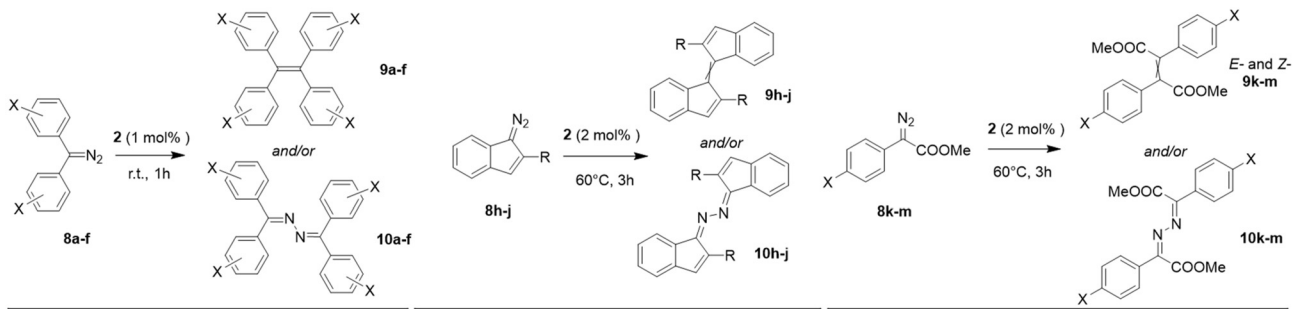

Entry	Substrate	Solvent	Product (isolated yield)
1	**8a**	$CDCl_3$	**9a** (95)
2	$(4\text{-}MeC_6H_4)_2CN_2$	C_6D_6	**10a** (86)
3	**8b**	$CDCl_3$	**9b** (92)
4	Ph_2CN_2	C_6D_6	**10b** (88)
5	**8c**	$CDCl_3$	**9c** (95)
6	$(4\text{-}MeOC_6H_4)_2CN_2$	C_6D_6	**9c** (95)
7[a]	**8d**	$CDCl_3$	**10d** (88)
8[a,c]	$(4\text{-}FC_6H_4)_2CN_2$	C_6D_6	**10d** (89)
9[b,c]	**8e**	$CDCl_3$	**10e** (90)
10[b,c]	$(4\text{-}BrC_6H_4)_2CN_2$	C_6D_6	**10e** (88)
11	**8f**	$CDCl_3$	n.r.
12	$(3,5\text{-}(CF_3)_2C_6H_3)_2CN_2$	C_6D_6	n.r.
13	**8g**	$CDCl_3$	**9g** (90)
14	fluorene	C_6D_6	**9g** (88)

Entry	Substrate	Solvent	Product (isolated yield)
15	**8h**	$CHCl_3$	**9h** (86)[d]
16	1-diazoindene	C_6H_6	**9h** (83)[d]
17	**8i**	$CHCl_3$	**10i** (90)
28	2-Me-1-diazoindene	C_6H_6	**10i** (89)
19	**8j**	$CHCl_3$	**10j** (92)
20	2-Ph-1-diazoindene	C_6H_6	**10j** (93)

Entry	Substrate	Solvent	NMR conversion (isolated yields) *E*-**9**	*Z*-**9**	**10**
21	**8k**	$CHCl_3$	47(42)	43(40)	10
22[b]	X = H	C_6H_6	45(40)	45(38)	10
23	**8l**	$CHCl_3$	45(36)	40(35)	10(7)
24[b]	X = Br	C_6H_6	35(30)	33(26)	13(8)
25	**8m**	$CHCl_3$	43(35)	37(30)	20(12)
26	X = MeO	C_6H_6	40(37)	35(30)	15(13)

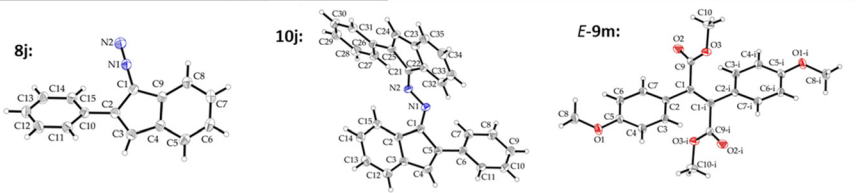

Fig. 4 Substrate scope of Mo-mediated homocoupling of diazo compounds and the selected crystal structures of the substrates or catalytic products. The general reaction conditions (catalyst loading, temperature and time) correspond to the schemes; the reaction was performed on a 0.5 mmol scale, the isolated yields are given in parentheses, and product identity and NMR conversion were estimated by ^{1}H NMR. [a] 3 hours of reaction time, [b] 24 hours of reaction time, [c] 60 °C reaction temperature, [d] the product consisted of a mixture of *E*,*Z*-isomers in *ca.* 2 : 1 ratio.

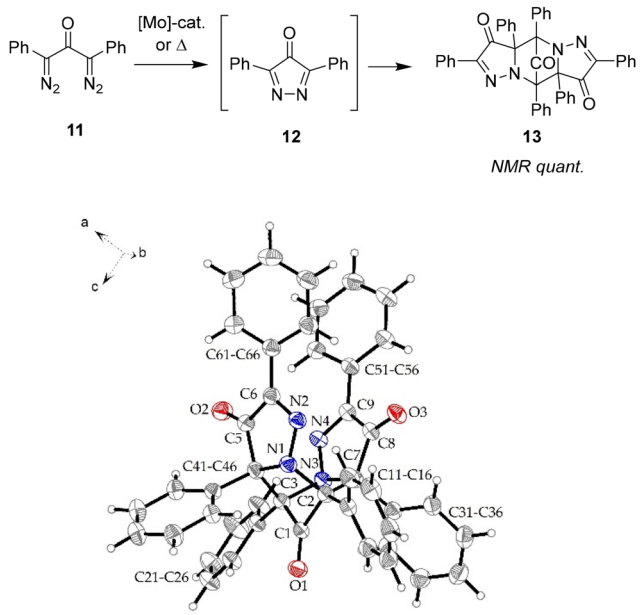

Fig. 5 The preparation and crystal structure of **13**.

acids.[24] The initial step involves the interaction of the transition metal centre with the diazo compound, leading to the formation of a metal–carbene intermediate (Fig. 6). This transformation represents a common entry point into the chemistry of highly reactive carbene species, and in numerous cases, such intermediates have been successfully intercepted and characterized.[31] The resulting carbene complex is then expected to undergo nucleophilic attack by a second molecule of the diazo compound. Depending on whether the nucleophile is the terminal nitrogen atom (N-nucleophile) or the carbon atom of the diazo compound (C-nucleophile), the reaction furnishes either an azine or an ethene derivative. The preference for C- *versus* N-nucleophilic attack is primarily governed by the electronic properties of the respective diazo compound, although to a certain degree the selectivity can be modulated by the polarity of the solvent.

Our attempts to perform the reaction under stoichiometric conditions and/or at lower temperatures did not result in the formation of a discrete carbene intermediate. In these experiments, either no reaction occurred or the homocoupling product was observed. These outcomes suggest that generation of a carbene intermediate represents the critical step, which is consistent with the thermodynamic data obtained in our previous work.[24]

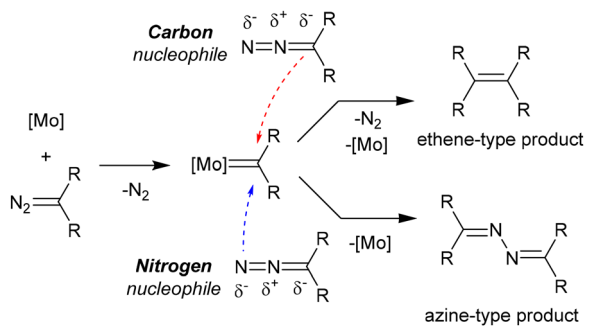

Fig. 6 Critical step for the formation of two possible products.

Conclusions

The synthesis, structural characterization, and catalytic applications of the borano–imido molybdenum(VI) complex are presented, as obtained from the reaction of a phenylpyridine-based boron azide with $[MoCl_4(thf)_2]$. Spectroscopic and single-crystal X-ray analyses confirmed a linear B–N–Mo linkage with significant electronic delocalization within the borane–imido fragment and a pseudo-octahedral coordination geometry. Coordination studies with neutral donors (bipyridine, dppe and triphenylphosphine) yielded structurally diverse Mo(V) derivatives, highlighting the adaptability of the borano–imido framework.

The borano–imido complex efficiently acts as a Lewis acid catalyst promoting the homocoupling of diazo compounds under mild conditions. For diaryldiazomethanes, product selectivity between tetraarylethylenes and azines was influenced primarily by the electronic nature of the substituents and, to a lesser extent, by the solvent. Electron-donating groups favored exclusive formation of tetraarylethylenes, whereas electron-withdrawing substituents led to selective azine formation. The complex also mediated the homocoupling of 1-diazoindenes and α-diazophenylacetates, with selectivity dictated by steric and electronic factors, yielding mixtures of ethylene-type and azine-type products.

Overall, this work establishes borano–imido molybdenum complexes as a new class of electronically distinctive and catalytically active imido species, expanding the scope of imido chemistry and offering new strategies for the homocoupling of diazo compounds.

Conflicts of interest

There are no conflicts to declare.

Data availability

Data supporting this article have been included in the supplementary information (SI). Supplementary information: complete experimental procedures, characterisation of the prepared compounds, copies of the NMR spectra, crystallographic parameters and additional structure diagrams. See DOI: https://doi.org/10.1039/d6dt00469e.

CCDC 2520309–2520319 contain the supplementary crystallographic data for this paper.[32a–k]

Acknowledgements

This work was supported by the Czech Science Foundation (project no. 23-06866S) and the Lumina Quaeruntur fellowship (project no. 200401) provided by the Czech Academy of Sciences. IR measurements were supported by the NanoEnviCz infrastructure (LM2023066), provided by the Ministry of Education, Youth and Sports of the Czech Republic. We thank Nina Hlávková for technical assistance with structure preparation.

References

1 D. E. Wigley, Organoimido Complexes of the Transition Metals, in *Progress in Inorganic Chemistry*, John Wiley & Sons, 1994, pp. 239–482.
2 (*a*) W. A. Nugent and B. L. Haymore, *Coord. Chem. Rev.*, 1980, **31**, 123–175; (*b*) R. R. Schrock, *Chem. Rev.*, 2002, **102**, 145–180; (*c*) R. R. Schrock, *Chem. Rev.*, 2009, **109**, 3211–3226.
3 P. Barrie, T. A. Coffey, G. D. Forster and G. Hogarth, *J. Chem. Soc., Dalton Trans.*, 1999, 4519–4528.
4 R. Schrock, *Angew. Chem., Int. Ed.*, 2006, **45**, 3748–3759.
5 K. Kawakita, B. F. Parker, Y. Kakiuchi, H. Tsurugi, K. Mashima, J. Arnold and I. A. Tonks, *Coord. Chem. Rev.*, 2020, **407**, 213118.
6 Y. Li, Y. Shi and A. L. Odorn, *J. Am. Chem. Soc.*, 2004, **126**, 1794–1803.
7 M. N. Cosio and D. C. Powers, *Nat. Rev. Chem.*, 2023, **7**, 424–438.
8 (*a*) K. Kawakita, E. P. Beaumier, Y. Kakuchu, H. Tsurugi, I. A. Tonks and K. Mashima, *J. Am. Chem. Soc.*, 2019, **141**, 4194–4198; (*b*) T. Akiyama, A. Yamamoto, T. Kasahara, T. Kusamoto and H. Tsurugi, *Organometallics*, 2025, **44**, 1047–1056.
9 (*a*) J. D. Lichtenman, S. C. Critchlow and N. M. Doherty, *Inorg. Chem.*, 1990, **29**, 439–442; (*b*) C. M. Jones, M. E. Lerchen, C. J. Church, B. M. Schomber and N. M. Doherty, *Inorg. Chem.*, 1990, **29**, 1679–1682; (*c*) A. Schorm and J. Sundmeyer, *Eur. J. Inorg. Chem.*, 2001, 2947–2955.
10 (*a*) For the P–N═[Mo] bond, see: G. Zhang, T. Liu, J. Song, Y. Quan, L. Jin, M. Si and Q. Liao, *J. Am. Chem. Soc.*, 2022, **144**, 2444–2449; (*b*) For the P–N═[W] bond, see: A. R. Cowley, J. R. Dilworth, A. K. Nairn and A. J. Robbie, *Dalton Trans.*, 2005, 680–693.
11 (*a*) A.-M. Fuller, W. Clegg, R. W. Harrington, D. L. Hughes and S. J. Lancaster, *Chem. Commun.*, 2008, 5776–5778; (*b*) A.-M. Fuller, D. L. Hughes, G. A. Jones and S. J. Lancaster, *Dalton Trans.*, 2012, **41**, 5599–5609.
12 C. Camp, L. N. Grant, R. G. Bergman and J. Arnold, *Chem. Commun.*, 2016, **52**, 5538–5541.
13 (*a*) M. F. Espada, S. Bennaamane, Q. Liao, N. Saffon-Merceron, S. Massou, E. Clot, N. Nebra, M. Fustier-Boutignon and N. Mézailles, *Angew. Chem., Int. Ed.*, 2018, **57**, 12865–12868; (*b*) T. Itabashi, K. Arashiba, H. Tanaka, K. Yoshizawa and Y. Nishibayashi, *Organometallics*, 2022, **41**, 366–373; (*c*) I. Benaissa, B. Rialland, S. Bennaamane, M. F. Espada, N. Saffon-Merceron, M. Fustier-Boutignon, E. Clot and N. Mézailles, *Angew. Chem., Int. Ed.*, 2024, **63**, e20242586.
14 (*a*) S. Bennaamane, M. F. Espada, A. Mulas, T. Personeni, N. Saffon-Merceron, M. Fustier-Boutignon, C. Bucher and N. Mézailles, *Angew. Chem., Int. Ed.*, 2021, **60**, 2021–20214; (*b*) S. Suginom, A. Okochi, T. Nakamura, A. Konomi, H. Tanaka, K. Yoshizawa and Y. Nishibayashi, *J. Am. Chem. Soc.*, 2025, **147**, 26684–26692.
15 K. Škoch, M. Buziková, D. Hnyk, M. Litecká, A. Vykydalová, D. Bavol, K. Lang and K. Kirakci, *Inorg. Chem.*, 2025, **64**, 18556–18566.
16 K. Škoch, M. Buziková, D. Hnyk, M. Litecká, M. Kloda, K. Kirakci and K. Lang, *Chem. – Eur. J.*, 2024, **30**, e202403263.
17 C. Y. Chou, J. C. Huffmann and E. A. Matta, *J. Chem. Soc., Chem. Commun.*, 1984, 1184–1185.
18 (*a*) L. Castellani and M. C. Gallazzi, *Transition Met. Chem.*, 1985, **10**, 194–195; (*b*) F. Stoffelbach, D. Saurenz and R. Poli, *Eur. J. Inorg. Chem.*, 2001, 2699–2703.
19 T. S. Pilyugina, R. R. Schrock, A. S. Hock and P. Müller, *Organometallics*, 2005, **24**, 1929–1937.
20 D. Rütter, M. van Gastel, M. Leutzsch, N. Nöthling, D. SantaLucia, F. Neese and A. Fürstner, *Inorg. Chem.*, 2024, **63**, 8376–8389.
21 C. Y. Chou, D. D. Devore, S. C. Huckett, E. A. Maatta, J. C. Huffman and F. Takusagawa, *Polyhedron*, 1986, **5**, 301–304.
22 Several polymorphs of dimeric $MoCl_5$ have been reported; for comparison, the β-$MoCl_5$ polymorph was selected; J. Beck and F. Wolf, *Acta Crystallogr., Sect. B*, 1997, **53**, 895–903.
23 (*a*) S. C. A. Sousa, I. Cabrita and A. C. Fernandes, *Chem. Soc. Rev.*, 2012, **41**, 5641–5653; (*b*) K. M. Dawood and K. Nomura, *Adv. Synth. Catal.*, 2021, **363**, 1970–1997; (*c*) J.-L. Wang, J.-T. Li, G.-Y. Wu and C.-X. Zhuo, *Trends Chem.*, 2024, **6**, 587–501.
24 M. Buziková, J. Schulz, M. Litecká and K. Škoch, *Inorg. Chem.*, 2026, **65**, 1408–1418.
25 (*a*) J. H. Hansen, B. T. Parr, P. Pelphrey, Q. Jin, J. Autschbach and H. M. L. Davies, *Angew. Chem., Int. Ed.*, 2011, **50**, 2544–2548; (*b*) M. Cui, S. Lin, H. H. Y. Sung, I. D. Williams, Z. Lin and G. Jia, *Organometallics*, 2019, **38**, 905–915.
26 (*a*) W. Baratta, A. Del Zotto and P. Rigo, *Chem. Commun.*, 1997, 2163–2164; (*b*) M. Basato, C. Tubaro, A. Biffis, M. Bonato, G. Buscemi, F. Lighezzolo, P. Lunardi, C. Vianini, F. Benetollo and A. Del Zotto, *Chem. – Eur. J.*, 2009, **15**, 1516–1526.
27 (*a*) C. Zhu, G. Xu, D. Ding, L. Qiu and J. Sun, *Org. Lett.*, 2015, **17**, 4244–4247; (*b*) P. K. Madarasi and C. Sivasankar, *Appl. Organomet. Chem.*, 2022, **36**, e6522.

28 S. Xie, Z. Yan, Y. Li, Q. Song and M. Ma, *J. Org. Chem.*, 2018, **83**, 10916–10921.
29 T. Bug, M. Hartnagel, C. Schlierf and H. Mayr, *Chem. – Eur. J.*, 2003, **9**, 4068–4076.
30 B. M. Trost and P. J. Whitman, *J. Am. Chem. Soc.*, 1974, **96**, 7421–7429.
31 H. A. Khan, M. Szostak and C. Sivasankar, *Org. Biomol. Chem.*, 2026, **24**, 734–766.
32 (*a*) CCDC 2520309: Experimental Crystal Structure Determination, 2026, DOI: 10.5517/ccdc.csd.cc2qll97; (*b*) CCDC 2520310: Experimental Crystal Structure Determination, 2026, DOI: 10.5517/ccdc.csd.cc2qllb8; (*c*) CCDC 2520311: Experimental Crystal Structure Determination, 2026, DOI: 10.5517/ccdc.csd.cc2qllc9; (*d*) CCDC 2520312: Experimental Crystal Structure Determination, 2026, DOI: 10.5517/ccdc.csd.cc2qlldb; (*e*) CCDC 2520313: Experimental Crystal Structure Determination, 2026, DOI: 10.5517/ccdc.csd.cc2qllfc; (*f*) CCDC 2520314: Experimental Crystal Structure Determination, 2026, DOI: 10.5517/ccdc.csd.cc2qllgd; (*g*) CCDC 2520315: Experimental Crystal Structure Determination, 2026, DOI: 10.5517/ccdc.csd.cc2qllhf; (*h*) CCDC 2520316: Experimental Crystal Structure Determination, 2026, DOI: 10.5517/ccdc.csd.cc2qlljg; (*i*) CCDC 2520317: Experimental Crystal Structure Determination, 2026, DOI: 10.5517/ccdc.csd.cc2qllkh; (*j*) CCDC 2520318: Experimental Crystal Structure Determination, 2026, DOI: 10.5517/ccdc.csd.cc2qlllj; (*k*) CCDC 2520319: Experimental Crystal Structure Determination, 2026, DOI: 10.5517/ccdc.csd.cc2qllmk.